EVLA Calibration at High Frequency

W. D. Cotton February 27, 2020

***Abstract*—Photometric calibration of connected element arrays such as the EVLA is generally based on observations of calibrators whose spectra and structures are known. This works well at low frequency and resolution where the calibrators are relatively compact and structural models adequate but works less well as the resolution increases and the sensitivity decreases with increasing frequency. An example of EVLA observations at 25, 32 and 41 GHz in "A" configuration is shown in which the traditional calibration produces very wrong results. An alternate calibration scheme based on imaging the calibrators rather than from their visibilities is shown to give much better results. Two photometric calibrators were included in the test data allowing a comparison of the results; they differed by 20% at 41 GHz. These issues will be even more serious for the ngVLA with its higher frequencies and longer baselines.**

***Index Terms*—calibration**

I. Introduction

PHOTOMETRIC calibration of radio interferometers at high frequency relative to lower frequencies is complicated by a number of factors 1) lower sensitivity, 2) larger and more rapid variations in the troposphere and 3) sparsity of stable, strong and compact photometric (amplitude) calibration sources. These become more problematic as the baselines become longer, hence at higher resolution. Of these problem areas, the lack of good photometric calibrators may be the most serious. Bright, compact sources at high frequencies tend to be blazars which are notoriously variable. Even thermal sources which are bright and stable are less than ideal as the are generally resolved at arc-second or higher resolution. The reliable calibrators used at GHz frequencies (3C48, 3C138, 3C286, 3C295...) are steep spectrum and resolved on baselines longer than a few km at frequencies about 10 GHz. Accurate structural and spectral models are available [1] and help in cases of moderate resolution but can give seriously erroneous results for the EVLA at 45 GHz in "A" configuration (~ 40 mas resolution).

This memo discusses some of the issues with traditional photometric calibration of the EVLA at high frequency and resolution and describes an alternate approach. An example of the calibration of an observations using the EVLA at 24–43 GHz in A configuration during the Summer is given using the Obit package [2] [1].

II. Traditional Photometric Calibration

The traditional technique for calibrating heterodyne interferometers operating at frequencies about 1 GHz is to use two, known calibration sources; a photometric and an astrometric calibrator. The photometric calibrator has a stable, or at least known, flux density and spectrum and need not be unresolved by the interferometer and need not have an extremely accurately known celestial position. The astrometric callibrator needs to have position known to much better than the resolution of the interferometer array and, preferably, be very small. Blazars make good astrometric calibrators as they tend to be very compact and bright but can have very substantial variations in brightness.

A. Two Calibrator Scheme

The traditional calibration approach [3] is to use observations of the two calibrators to infer the flux density and spectrum of the astrometric calibrator at the time of the observation and then use the astrometric calibrator to calibrate both amplitude and phase.

B. SetJy,Calib,GetJy Calibration

One scheme used by traditional packages like the one described in [3] consists of the following:

1) **SetJy**. This program has parameterized model spectra for the primary photometric calibrators and is used to compute calibrator flux densities as a function of frequency.
2) **Calib**. Given models of the calibrators, usually a point for the astrometric source and structural/spectral models for the photometric calibrator, calculates complex gains for each calibrator as a function of antenna, polarization, time and frequency.
3) **GetJy**. This program uses the fitted gains and the assumed flux densities and calculates the spectrum of the astrometric calibrator and corrects the amplitude of the gains for any change to the assumed spectrum.

This scheme depends on adequate SNR and calibrator models that accurately reproduce the observed visibilities. The spectrum fitting uses the ratio of potentially noisy gain measurements and may not be very stable.

GetJy estimates the spectra of one or more astrometric calibrators using the ratio of calibration gain amplitudes to one or more amplitude calibration sources with know structure and spectra. For each antenna and Spectral Window (AKA "IF") for each photometric or astrometric calibrator, s, the ratio of assumed flux density to gain amplitude squared is given by:

$$R^s_{ant,IF,pol} \;=\; \left\langle \frac{flux}{amp^2} \right\rangle_{time}$$

where $\langle\ \rangle_{time}$ is the expectation of a set of time samples; in the simple case, an average. Each antenna and spectral window has a calibration factor

$$r^{cal}_{ant,IF,pol} \;=\; \left\langle R^{cal}_{ant,IF} \right\rangle_{cal}$$

National Radio Astronomy Observatory, 520 Edgemont Rd., Charlottesville, VA, 22903 USA email: bcotton@nrao.edu

[1] http://www.cv.nrao.edu/∼bcotton/Obit.html

derived from all photometric calibrators. The flux density of astrometric calibrator a in each spectral window IF is derived using the antenna and polarization samples:

$$flux^a_{IF} = \left\langle r^{cal}_{ant,IF,pol} \times R^a_{ant,IF,pol} \right\rangle_{ant,pol}$$

Finally a two term spectrum (flux density at the reference frequency and spectral index) is fitted. This spectrum is evaluated at each spectral window reference frequency to obtain the flux density in that spectral window.

C. High Frequency Adaptations

For noisy, low SNR data for which the atmospheric variations are small and slow compared to the averaging time, vector averaging of data gives optimal results. In the case of high SNR but large and rapid variations in atmospheric phase, the amplitudes are more stable than the phases and the "ampscalar" scheme may be useful. This averages data going into solutions by amplitude and phase separately rather than a vector average. Neither ampscalar nor vector averaging work particularly well when the SNR is low and the phase variations large and fast.

Longer baselines have higher resolution and are more sensitive to the spatial structure. Limiting the range of baseline lengths of the data going into calibration solutions can reduce the sensitivity to incompletely modeled source structure at the cost of lower SNR in the solutions. For calibrators that are marginally resolved, this technique may remove the need for accurate calibrator models. Limiting the uv range going into gain solutions can also deal with the case of marginally sampled very large scale structure around the source.

III. Example Traditional Failure

Examples of where this process goes wrong are from a Summer, night time observation using the EVLA in A configuration at 25, 32 and 41 GHz using 3C48 and 3C138 as photometric calibrators and the unresolved flatish spectrum source J0239-0234 as an astrometric calibrator. Observations cycled among the observing bands with fast switching between J0239-0234 and the target. One 10 minute scan was performed on each 3C48 and 3C138 at each frequency. Calibrator spectra were taken from [4]. The standard calibration gave the target an implausibly inverted spectrum. When the calibration was repeated using ampscalar averaging there was little change in the results.

A. Initial Calibration

The two flux density calibrators used are both significantly resolved in these observations. Figure 1 shows images of 3C48 and 3C138 at 43 GHz as observed by the EVLA in A+C configuration showing the very extended nature of the sources. In an attempt to reduce the effects of calibrator resolution, all but the shortest baselines were excluded in deriving the flux density of the astrometric calibrator; this produced only minor improvements.

The fundamental problem was revealed by examining the results of this calibration on the photometric calibrator data

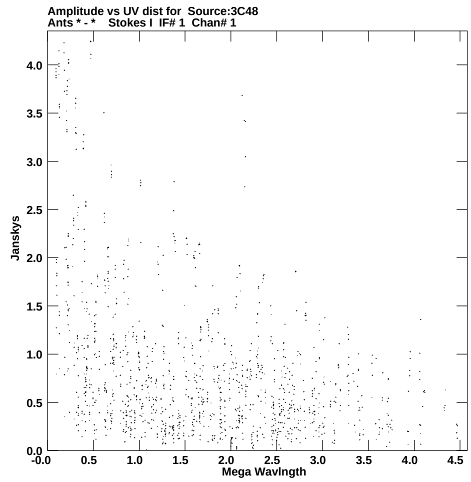

Fig. 2. Distribution of visibility amplitudes of the 3C48 43 GHz data vs. baseline length after calibration as described in Section II-B. Note, the correct total flux density is 0.61 Jy.

TABLE I
STANDARD CALIBRATION

source	Frequency GHz	True Jy	Integrated Jy
J0238-0234	25	0.37[1]	0.56
J0238-0234	32	0.31[1]	1.18
J0238-0234	41	0.31[1]	1.78
3C48	25	1.085	1.62
3C48	32	0.770	2.63
3C48	41	0.565	1.43
3C138	25	1.029	1.35
3C138	32	0.753	2.54
3C138	41	0.575	3.50

[1] from calibration in Section V.

themselves. A plot of the visibility amplitudes as a function of baseline length for the 43 GHz data is displayed in Figure 2. "Calibrated" amplitudes in excess of 4 Jy are seen whereas the integrated flux density is 0.61 Jy. Similar effects were also seen at lower frequencies but decreasing in severity with decreasing frequency. This effect led to the very incorrect results for the target. This function of frequency is due to the decreasing SNR of the data with increasing frequency due to 1) the steep spectrum of the calibrators, 2) the increasing noise of the receivers and 3) the increasing resolution of the calibrators. Use of a model of the calibrators could not compensate for the increasingly noisy data.

A comparison of the integrated flux densities derived from imaging data using this standard calibration to the "True" values is given in Table I. "True" values for 3C48 and 3C138 are from [4] and for J0238-0234 are those derived from the analysis in Section V.

B. Improved GetJy

The calibration results described in Section III-A used a simple averaging expectation operator as outlined in Section II-B. This is optimal for high SNR, well behaved data but is sub-optimal for noisy, poorly behaved data. The expectation operator was changed to a more robust, median averaging; the

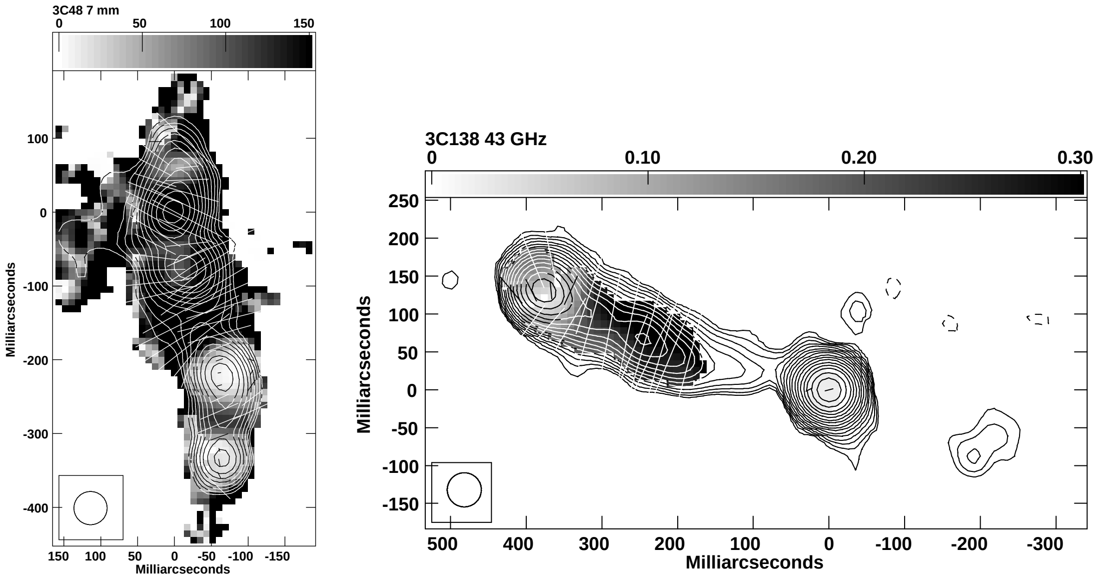

Fig. 1. **Left**) 3C48 at 43 GHz, Stokes I is shown in contours, linear polarization E vectors are given as lines and the fractional polarization is given as the inverted gray scale with a scale bar at the top.
Right) same as Left but 3C138.
The length of the vectors are proportional to the polarized intensity. Contours are at powers of $\sqrt{2}$ times 2 mJy/beam. The circle in the lower left corner gives the size of the resolution and the "core" of 3C48 is the bottom most component and in 3C138 is the component at position (0,0). From [5].

TABLE II
IMPROVED GETJY

source	Frequency GHz	True Jy	$\sum$CC Jy	Integrated Jy
J0238-0234	41	0.31[1]	1.66	1.66
3C48	41	0.565	3.35	3.52
3C138	41	0.575	3.50	3.49

[1] from calibration in Section V.

list of values is sorted, the extreme 25% on each end of the distribution discarded and the middle 50% averaged. This is much less sensitive to outlyers than simple averaging but gives better sensitivity than a simple median.

This version was tested on the 41 GHz data which are the most problematic in Section III-A. The principle result of this calibration is the fitted spectrum of the astrometric calibrator. Using simple averaging the fitted flux density is 1.78 Jy and spectral index=0; using the median average flux density is 1.68 Jy, spectral index=-0.3. As will be shown in Section V, the correct flux density is ~ 0.31 Jy. The results of imaging the 41 GHz calibrators is given in Table II. The improved GetJy does not result in calibration significantly better than the original version. The fundamental calibration problems do not seem to be due to the noisy calibration fits and are likely due to the strong resolution of the photometric calibrators and a less than perfect model.

IV. Alternate Calibration

An alternative approach that does not depend on having extremely precise photometric calibrator models but merely knowing the total flux density spectrum of the calibrator is to first assume an initial spectrum for an astrometric calibrator. The data is then trial calibrated using this spectrum, with the photometric calibrators treated as targets. All calibrators and targets are imaged and the ratio of the true flux density to the total in the image of the photometric calibrators is the factor by which the calibration is in error ("calibration factor"). The sum of the CLEAN components or box integrals (e.g. tvstat) around the source give estimates of the image total flux density. The images generated from this trial calibration are multiplied by the calibration factor derived from the photometric calibrator images. This method requires no prior knowledge of the photometric calibrators except the total flux density, as seen by the array.

V. Example Alternate Calibration

The calibration scheme discussed in Section IV was applied to the data discussed in Section III-A. The trial spectrum for the astrometric calibrator was 0.5 Jy and a flat spectrum. The results of the calibrator imaging are shown in Table III. Calibration correction factors were derived from the average of the two photometric calibrators using the sum of the CLEAN components and are 0.73 (25 GHz), 0.61 (32 GHz) and 0.64 (41 GHz). Table III shows residual calibration errors of order 20% at 41 GHz for 3C48 and 3C138 which is much better that the wildly erroneous results in Table I. This calibration also gives plausible results for the target source.

VI. Discussion

At high frequency and resolution there is a paucity of stable, compact photometric calibrators for arrays such as the EVLA. The standard calibrators such as 3C48, 3C138, 3C147 and 3C286 are steep spectrum-ed with sizes of the order of 0.5". These are weak and strongly resolved at the top ranges of frequency and resolution for the EVLA. Even

TABLE III
ALTERNATE CALIBRATION

source	Frequency GHz	True Jy	$\sum$CC Jy	Integrated Jy	corr $\sum$CC Jy
J0238-0234	25	0.37[1]	0.500	0.500	0.37[1]
J0238-0234	32	0.31[1]	0.500	0.500	0.31[1]
J0238-0234	41	0.31[1]	0.502	0.506	0.32[1]
3C48	25	1.085	1.49	1.52	1.09[1]
3C48	32	0.770	1.17	1.05	0.71[1]
3C48	41	0.565	0.74	0.85	0.47[1]
3C138	25	1.029	1.39	1.39	1.05[1]
3C138	32	0.753	1.34	1.25	0.82[1]
3C138	41	0.575	1.10	1.10	0.70[1]

[1] after applying calibration factor.

with detailed structural and spectral models, these calibrators are shown to produce very inaccurate calibration with the traditional SetJy/Calib/GetJy method. An alternate method of deriving the fundamental calibration from imaging of the calibrators rather than from the visibilities is shown to give more stable results. Since the test dataset contained two similar photometric calibrators, the consistency of the results could be compared. At 41 GHz the two calibrators gave results differing by 20%. This issue will be even more serious for the ngVLA which will operate at higher frequencies and on longer baselines.

REFERENCES

[1] W. D. Cotton, “Interferometry Wideband, Widefield Calibrator Models,” *Obit Development Memo Series*, vol. 38, pp. 1–6, 2014. [Online]. Available: ftp://ftp.cv.nrao.edu/NRAO-staff/bcotton/Obit/CalModel.pdf

[2] W. D. Cotton, “Obit: A Development Environment for Astronomical Algorithms,” *PASP*, vol. 120, pp. 439–448, 2008.

[3] W. D. Cotton, “EVLA Continuum Scripts: Outline of Data Reduction and Heuristics,” *Obit Development Memo Series*, vol. 29, pp. 1–25, 2012. [Online]. Available: ftp://ftp.cv.nrao.edu/NRAO-staff/bcotton/Obit/EVLAObitScripts.pdf

[4] R. A. Perley and B. J. Butler, “An Accurate Flux Density Scale from 50 MHz to 50 GHz,” *ApJS*, vol. 230, p. 7, 2017.

[5] W. D. Cotton, E. Kravchenko, Y. Y. Kovalev, and E. Fomalont, “Search for extreme rotation measures in CSS sources,” *Astronomische Nachrichten*, vol. 337, p. 87, 2016.